HYDROACOUSTIC ESTIMATION IN HIGH DENSITY FISH SCHOOLS

Dean W. Lytle, Professor
Douglas R. Maxwell, Research Assistant
Electrical Engineering Department
University of Washington
Seattle, Washington

INTRODUCTION

Hydroacoustic biomass abundance estimation is generally performed under the assumption of "first-order" scattering in which each fish in a school is assumed to receive and return acoustic signals as if no other fish were present. Although in most assessment environments this assumption is acceptable, high density schools do occur where first order scattering cannot be assumed. Multiple scattering and attenuation of the incident intensity have a profound effect on the received energy when school density, or school extent, or fish size grow large. Both multiple scattering and attenuation are predicted and their effect calculated by scattering theories, and have been observed to some extent during ocean surveys. Experimental verification of these effects under controlled conditions (as reported in the following pages) enable identification of the mechanisms responsible and postulation of the requirements for a more accurate estimation scheme.

THEORETICAL ASPECTS

In Fig. 1. we illustrate an incident acoustic plane wave with direction vector $\hat{i}$ (which can be specified by - two angles, θ_i and ϕ_i). We assume the incident wave to be narrow enough in bandwidth to be considered a single frequency. This wave is scattered by the scatterer (fish) at the origin, and thus, the pressure at the point (r, θ_o, ϕ_o) consists of the sum of the incident wave, p_i, and the scattered wave, p_s. The scattered wave can be represented as

$$p_s(r, \theta_o, \phi_o) = \frac{e^{jkr}}{r} f(\hat{o}, \hat{i})\, p_i(0) \tag{1}$$

where $p_i(0)$ is the incident pressure at the scatterer, $k = 2\pi/$ wavelength is the wave number, $f(\hat{o},\hat{i})$ is the complex scattering amplitude of the fish, and Eq.(1) is written in complex form with the time variable $e^{j\omega t}$ suppressed. Note that the complex scattering amplitude is a function of both the incident direction, $\hat{i}$, and the receiving direction, $\hat{o}$, as well as the type and size of fish and the signal (radian) frequency, ω.

A more measurable scattering function is the differential scattering cross-section, σ_d.

$$\sigma_d(\hat{o},\hat{i}) \triangleq c_d \mid f(\hat{o},\hat{i})\mid^2 \tag{2}$$

The constant c_d depends on the units being used and is such that σ_d is an area. Thus, if I_i is the incident intensity (in power/unit area) at the scatterer, then at unit distance from the scatterer in the direction o, the scattered intensity is

$$I_s = I_i\, \sigma_d \tag{3}$$

The backscattering cross-section, σ_b, is simply the differential scattering cross-section for the special case, of $\hat{o} = -\hat{i}$.

$$\sigma_b = \sigma_d\ (-\hat{i},\hat{i}) \qquad (4)$$

The primary scattering structures of a typical semi-pelagic fish are the swim bladder, which is virtually 100% reflective because it is gas-filled, and the backbone complex, which may not be a negligible contributor for wavelengths small compared to fish size. Because of the shapes and location of these organs, aspect angle strongly affects values for σ_b. Broadside aspect values are usually 2-5 times larger than those for dorsal incidence, [1]. This quantity, illustrated in Fig. 2, has been measured for several species, sizes, and fish orientations (but usually dorsal incidence). The results, however, are not uniform, being strongly dependent on species and frequency range used.

It will be useful to define another scattering measure; the extinction cross-section, σ_t, represents the total power removed from the incident wave.

$$I_i\ \sigma_t = \text{power scattered} + \text{power absorbed} \qquad (5)$$

Note that $\sigma_t(\hat{i})$ is a function of the incident wave direction. There appears to be no record of measurements of σ_t for fish.

Optical Density

The exact analytic determination of the scattered pressure field or intensity at the receiver due to a random collection of scatterers (fish) is extremely difficult. There exist several approximation techniques which are valid for limited types of scattering volumes. The classification of types is based on a quantity called the optical density, τ, which is proportional to numbers density, extinction cross-section of individual scatterers (dependent on their size and orientation), and the vertical extent of the occupied volume, or school. Each of these factors contribute increasingly to the disturbance of the incident wave.

To see how the optical density is determined in theory, consider Fig.3. In that figure a plane wave propagates through a rectangular volume with unit area normal to the direction of propagation. As the wave progresses in the z-direction the accumulated extinction cross-sectional area it has intercepted within that volume increases monotonically. The optical density is defined as the expected value of this accumulated area.

$$\tau(z) = E\,[\text{accumulated } \sigma_t] = \int_0^z \int_w \sigma_t(w)\, n\,(z,w)\, dwdz \qquad (6)$$

The term $n(z,w)$ is numbers density of fish of size w at the depth z.* The extinction cross-section $\sigma_t(w)$ is a function of the size w. Note that if the fish have uniform density (ρ) and size throughout the volume then

$$\tau(z) = \rho\sigma_t z \qquad (7)$$

We shall be concerned here principally with two receiver locations: 1) at the transmitter (backscattering), and 2) at a point beyond the scattering volume, directly in front of the transmitter (line of sight transmission).

Tenously distributed (low density) schools. If $\tau(z_b) << 1$ (where z_b is the bottom of the school), then the school is tenuously distributed and the energy incident on any fish (as well as that backscattered) is assumed to be unaffected by the presence of others. This is the single scattering, or Born, approximation. For backscattering, the received power can be integrated, and if certain statistical properties are assumed and the distribution of σ_b is known, an estimate of the numbers density for a particular volume may be extracted (echo integrator) [2]:

$$\hat{\rho} = \frac{\overline{I_o}}{K\overline{\sigma}_b} \qquad (8)$$

* The size as used here is the effective acoustical size which includes orientation, etc.

$\overline{Io}$ is the average intensity computed by integrating the square of the received voltage over a time increment, $\overline{\sigma}_b$ is the average backscattering cross-section, and K represents all system gains and transducer calibration values. For the line-of sight case, we obviously expect no change in reception due to the presence of fish.

Medium density schools. For somewhat denser fish ($\tau \lesssim 1$) we can approximate the intensity at a point within the scattering volume by the incident intensity reduced by the energy-removing properties of intervening fish. It is not difficult to show that if the total power removed from the incident wave (represented for each fish by its σ_t) does not reappear, then the intensity at depth z is

$$I(z) = I_o(z)e^{-\tau(z)} \tag{9}$$

where $I_o(z)$ is the acoustic intensity that would be present with no fish. This is the first order multiple scattering approximation ($1^{\underline{st}}$ O.M.S.). It could also be called the pure attenuation model. This approximation makes the reasonable assumption that the uncertainty in location of any fish is at least a wavelength (randomly distributed) so that simple addition of intensities may be used rather than working with phase-sensitive amplitudes.

To compute the received backscatter power, consider Figure 4 where the geometry of the situation is illustrated. The fish school contained in volume V_s is assumed distant enough so that the incident acoustic wave can be considered plane. The school will be assumed large and uniform enough so that the optical density is a function of r and not of the angles θ and ϕ. The returned power is obtained by integrating the backscatter from each incremental volume with the only modification from standard being the two way attenuation $e^{-2\tau(r)}$ due to the $1^{\underline{st}}$ O.M.S. approximation.

$$P_r(t) = \int_{V_s} \frac{A^2(t - \frac{2r}{c})\, G_t(\theta,\phi) G_r(\theta,\phi)}{r^4} \bar{\sigma}_b(V) e^{-2\tau(r)} dV(r,\theta,\phi) \qquad (10)$$

$A^2(t - \frac{2r}{c})$ = delayed squared pulse waveform

G_t & G_r = transmitter & receiver beam gain functions

$\bar{\sigma}_b(V)$ = backscatter density [$\sigma_b(V)dV$ = backscatter cross-section in the volume dV]

The line-of-sight case is somewhat more complex in that the received signal consists of a direct component and a scattered component depending upon the differential scattering cross-section. The received power (for continuous rather than pulsed transmission) is given by the following expression and the geometry illustrated in Fig.5.

$$P_r = P_o \left\{ \frac{e^{-\tau(r_1+r_2)}}{(r_1+r_2)^2} + \int_{V_s} \frac{G_t(\theta_1,\phi)}{r_1^2} e^{-\tau(r_1)} \bar{\sigma}_d(\theta_1,\phi,\theta_2,r_1) \frac{G_r(\theta_2,\phi)}{r_2^2} e^{-\tau(r_2)} dV \right\} \qquad (11)$$

{ $\bar{\sigma}_d(\theta_1,\phi,\theta_2,r_1)$ is the differential scattering cross-sectional density which depends on numerical and size densities and also orientation. }

In Eq. (11) we have made the assumption that transmitter and receiver are far enough from the insonified scatterers that plane wave assumptions hold and $r_1+r_2=r$ the range between transducers.

Higher density schools. As the optical density becomes larger ($\tau \gtrsim 1$ and $\tau>>1$) the scattered energy cannot be neglected when considering the incident intensity at any scatterer. That is, a significant amount of the acoustic energy arriving at any fish will have already been scattered from intervening fish. For this situation the 1st O.M.S. expressions of Eqs. (10) and (11) will no longer be valid.

At the present time there seems to be no adequate analytic approximation which will be valid for this situation when $\tau \gtrsim 1$. However, when $\tau >> 1$ a diffussion approximation may be appropriate. The diffusion approximation is the result of treating this acoustic problem using methods of transport theory [3]. Generally speaking, transport theory develops equations for the flow of power when waves are propagated through random media. Any detailed discussion is beyond the scope of this paper, but some insight can be gained by examining Fig. 6.

In Fig. 6a we illustrate a hypothetical school of fish in a layer from a to c with a receiver at the transmitter for backscatter measurements in the pulse mode and another receiver below the layer for line-of-sight measurements in the cw mode. To the left we show the optical density, $\tau(z)$, which for a constant density school increases linearly through the layer. In Fig. 6b, we illustrate the power received at the lower receiver as a function of the optical density at the lower edge of the layer (τ_c). The upper curve is the single scattering (Born) approximation which simply assumes the line-of-sight power unaffected by intervening fish and hence is independent of τ_c. The lower curve is the 1^{st} O.M.S. approximation obtained from Eq. (11). The dashed curve would be the actual power received with the tail section analytically obtainable from the diffusion approximation.

Figure 6c shows the backscatter power received from the small layer between b and c for the various approximations. In the latter half of this paper we discuss experimental results which verify the theory discussed above.

EXPERIMENTAL PROCEDURES

The experimental work was conducted at an aquaculture facility operated by the Weyerhaeuser Co. near Olympia, WA. Net-enclosed confinement pens containing known numbers of a particular salmon species of uniform size were available for our measurements. The fish ranged from 12 to 36 cm. in length and numbers from 900 to 20,000. Due to tidal motion, circular swimming patterns, weather, time of day, etc., the distribution within the pens was usually very non-uniform. In heavily populated pens, spatial density extended from zero to nearly $1000/m^3$. Empty pens were also available for testing with controlled numbers of fish.

Figures 7 and 8 illustrate the physical arrangement, data collection and processing techniques and sample waveforms for line-of-sight and backscatter experiments. In the line-of-sight case, 267 kHz (wavelength = 0.53 cm) continuous signal was applied to the upper transducer and the transmitted pressure received by the lower one. Each sample of the processed waveform was stored according to its voltage level, resulting in a histogram of the amplitude of the transmitted envelope.

In the backscattering mode, the side-looking transducer was used. A sinewave burst of pulse length 0.2 msec (containing 53 cycles) was transmitted from outside the pen at a repetition rate of 2/sec. The received signal was amplified by a time-varying gain (TVG) to account for the spherical spreading loss. The final output from the integration routine yields the backscattered energy from a pre-selected range (volume) increment. These increments were generally chosen small (0.2 - 0.5 m) due to the highly non-uniform density within the pens. The results could then be compared to the expected received energy in the single scattering approximation to determine the degree to which higher-order effects were encountered.

Line-of-sight transmission results. First, a single fish (identified visually and by tape records) which traverses the acoustic beam results in a signal fluctuation illustrated in Fig. 9. The computed histogram of received signal levels is spread and its mean level lowered a slight amount, depending on the duration of sampling and the fish velocity and position in the beam. This figure also shows the effect of bistatic scattering in the forward direction.

Figure 10 shows received power level distributions of sampled data for 0, 11, 100, 230, and 300 fish in a small pen. Their average size was 7 fish per kg. and about 23 cm in length. The effective occupied volume had to be crudely measured, because it changed somewhat as more fish were added, so that the number per unit volume could only be approximated. Table I summarizes some of the more important statistical features of the transmission samples. Note that with increasing density the mean power levels decline, and the spread of the envelope increases. The variance of the normalized histograms began to decrease here at a density of $130/m^3$. In survey tests described below (see Fig. 11), whenever the density (of somewhat smaller fish) exceeded $200/m^3$ or so, the histogram outline become a smooth, Rayleigh-like probability density function whose mean decreased as the numbers grew larger, as virtually all of the transmitted power was concentrated at a much reduced level.

Samples received at levels greater than the clear water mean are due to energy returned to the system via additive forward scattering. This effect undoubtedly occurs at lower transmitted voltage levels as well, but without knowledge of the complete differential scattering cross-section σ_d of individual fish, the quantitative increase of power at the receiver is incalculable [i.e., the integral in Eq. (11)].

The dorsal incidence extinction cross-section for a large fish (large meaning kb >> 1, where b is the smallest linear dimension of the scatterer) is roughly $2\sigma_b$. For a 23 cm. fish, Love's universal equation [1] for dorsal incidence backscattering cross-section gives

$$2\sigma_b = .043L^{1.91}\,\lambda^{.09} \times 2 = 32.2 \text{ cm}^2 \qquad (12)$$

and Goddard and Welsby's several-species results [4] gives

$$2\sigma_b = .0039\,L^{2.58}\,\lambda^{-.58} \times 2 = 34.8 \text{ cm}^2 \qquad (13)$$

where, for each L is the fish length in meters and λ is the wavelength in meters. The values of σ_t measured from each point in the controlled tests yields an average σ_t of 28 cm^2, which is lower than the above values, due either to species or to our neglect of the forward scattering.

At any rate, it is obvious from these test that there exists marked attenuation of the transmitted signal as it passes through the scattering volume, even for those relatively low densities. It is also evident that the transmission coefficient declines nearly exponentially with increasing density, as predicted.

Survey trials were also conducted in large pens full of fish. By locating the transducer system at many points within the pens (Fig. 11), horizontal profiles of the average transmission levels were obtained. From these, the corresponding densities and total numbers estimates were procured by using only the first term in Eq. (11) (which biases the estimate to the low side, theoretically). Even using the lowest reasonable values for σ_t, the numbers estimates were at least 30% low, implying that use of the mean attenuation alone is not an adequate basis for estimation, and that at least first-order multiple scattering is taking place.

Backscattering results. Estimation by the echo integration technique requires a knowledge of the mean backscattering cross-section of the fish.

In the usual applications, this cross-section would be for dorsal aspect. In our case, the transmitter was pointed horizontally so the applicable σ_b varied from broadside to head or tail aspect. Our measurements and calculations indicated that the broadside σ_b was approximately 1.5 times the dorsal σ_b values for several species reported by Goddard-Welsby.

Only the fish insonified across the center of the pen were viewed in near-broadside aspect. Other transducer locations produced the problem of determining $E[\sigma_b]$ for non-broadside orientation of the fish. Figure 12 exhibits typical outputs for side-viewing data taken from two locations. Arrows indicate sections where the densities should have been nearly equal, as judged from transmission loss results over those volumes. This implies that average σ_b for near end-on incidence is considerably lower than the values estimated above. For intermediate transducer positions, the output for comparable densities ranged between those shown in Fig. 12. In order to make the computed densities match at corresponding points in Fig. 12c, it is necessary to assume a reduction in backscattering cross-section to about one quarter its broadside value. (In this argument, no account is taken of attenuation or forward scattering.)

After surveying the entire volume of several pens, total numbers estimates were obtained by three methods; I used the integrator output only, II used output corrected for non-broadside incidence as described above, and III used only the output for energy returned out to halfway across the center of the pen at various depths. The last method relied heavily on the circularly symmetric horizontal distribution within most of the pens, as measured by line-of-sight tests. This technique actually yielded the best estimates because only the optical distance to the center of the pen contributed to attenuation and because the need to guess σ_b for odd aspect angles was elimi-

nated. The results of three such surveys are shown in Table II. Note that the estimates improve as the biomass decreases, although in all cases $\hat{N}$ was too low.

In an effort to correct the echo integrator output, each incremental volume density estimate was multiplied by a coefficient inversely proportional to the expected transmission decline due to attenuation in the intervening increments. Unfortunately, the factor $e^{2\tau}$ overcompensated as τ approached 0.2, a value exceeded at some range in nearly all our trials.

Other tests provided much stronger evidence for the existence of multiple scattering, again in amounts proportional to the biomass and spatial extent of the scattering media. Figure 13 shows the location of an empty plastic bottle with and without intervening fish. The apparent distance to this strong target is greater when fish are present, even though the actual distance was carefully measured to be identical in each case. Also, those returns viewed on an oscilloscope showed the target to be changing position with each pulse, and this was evident in the spread out behavior of its processed "position." (The target strength difference in the figure was due to a slight orientation change of the target.) The same tests conducted using a much greater intervening biomass amplified this effect. At the time of TVG cutoff (6 m) returns from fish near the end of the large pen (Fig. 14) had not yet returned, much less any signal from the target bottle. This pen appeared to have uniform circular symmetry, implying that the far-ranged returns which were received had been considerably attenuated, also.

A valid argument can be forwarded that multiply scattered signals which find their way to the target and back necessarily follow a longer path than the undisturbed signal. This effect was directly observable in high density smaller pens, where signals appear to have been reflected from the clear water beyond the far range of the pens (Fig. 15). This was noted in all high

density ($\tau \lesssim .5$) trials, and the amount of delayed power (shaded) seemed to increase with τ, but too few results were obtained with small pens to draw any quantitative conclusions.

CONCLUSIONS

The assumption of a linear relationship between the energy reflected from a group of scatterers and their biomass and spatial extent has been predicted and shown here to deteriorate as the optical density increases. Directly measured attenuation in transmission mode experiments, coupled with evidence of attenuation in various backscattering mode tests, shows conclusively that "shadowing" is indeed present, even for low densities.. Multiple scattering phenomena are exhibited by the fact that, in the higher densities encountered in this work, attempts to account for attenuation were not adequate to explain the amounts of power received in either mode of operation. Further, the delay in return times causes an energy smearing effect attributable to the increased path lengths of acoustic signals which are multiply scattered within the population volume. Each of the above effects is predicted to exist in quantities governed by the optical density of the medium.

Because of the errors involved and inherent crudeness of our pulse estimation scheme, the exact extent of these effects on assessments of dense populations of fish was here incalculable. The output of the echo integrator cannot be properly related to a density estimate without a more accurate appraisal of the various cross-sections required to define a high-density model. These include the backscattering cross-section σ_b, the extinction cross-section σ_t, which is vital in accounting for attenuation through high densities, and the differential cross-section $\sigma_d(\hat{o},\hat{i})$, which must be known for consideration of multiple scattering, particularly in the forward direction.

The problem of estimating density from echo records, if we are faced with an energy vs. optical density picture like that in Fig. 4 (and Rottingen's [6] work suggests that indeed we are), at first glance appears to imply that the yet-undiscovered inversion technique we seek may not give a unique answer. However, in actual field use, the optical density can be found by processing small intervening range increments first, and adding these $\Delta\tau$'s, since this value can only increase with depth, so that step-by-step checking can be used to determine the side of the reflected energy maximum that $\hat{\rho}$ lies on. The solution can be found, if the appropriate form of processing is used for a given τ. The key ingredients necessary to realize thse improvements (i.e., the aforementioned scattering parameters) are still lacking. Work is now in progress to measure these parameters.

TABLE I

Statistics of line-of-sight power level histograms

	Number of fish (Density-fish/m^3)				
	0(0)	11(11)	100(60)	230(100)	300(130)
Mean	16.7	16.6	14.6	13.7	11.7
Max. spread	7	10	36	43	45
Standard deviation	.75	1.2	7.4	9.6	8.4
% of samples below clear water value	0	7	45	60	69

TABLE II

Estimation of densities

Number	Size	Assumed σ_b	Method	$\hat{N}$	% Error
19525	9.7/kg. 23 cm.	30 cm^2	I	6,900	65
			II	11,500	41
			III	15,800	21
5049	4/kg. 30 cm.	48 cm^2	I	2,050	59
			II	3,600	29
			III	4,200	17
950	117/kg. 11 cm.	4 cm^2	I	600	37
			II	820	14
			III	850	11

REFERENCES

[1] Love, R. H., "Maximum Side-Aspect Target Strength of an Individual Fish", JASA, Vol. 46, pp.746-751, 1969.

[2] Ehrenberg, J. E., "Echo Integrator Analysis", notes for extension course in fisheries acoustics, University of Washington, 1973.

[3] Ishimaru, A., Wave Propagation and Scattering in Random Media, Vol.1, Academic Press, N.Y., 1978.

[4] Goddard, G. C. and Welsby, V. G., "Statistical Measurements of the Acoustic Target Strength of Live Fish", submitted at Symposium on Acoustic Methods in Fisheries Research, No. 40.

[5] Maxwell, D., "The Effects of Higher-order Scattering Phenomena on Abundance Estimates of High Density Fish Populations", M.S. Thesis, University of Washington, 1977.

[6] Røttingen, I., "On the Relation Between Echo Intensity and Fish Density", Fisk Dir. Skr. Ser. Hav Unders, 1976.

[7] Crispin, J. W. Jr., and Maffett, A. L., "Radar Cross-section Estimation for Simple Shapes", Proc. of IEEE, Vol. 53, No. 8, pp. 833-848, 1965.

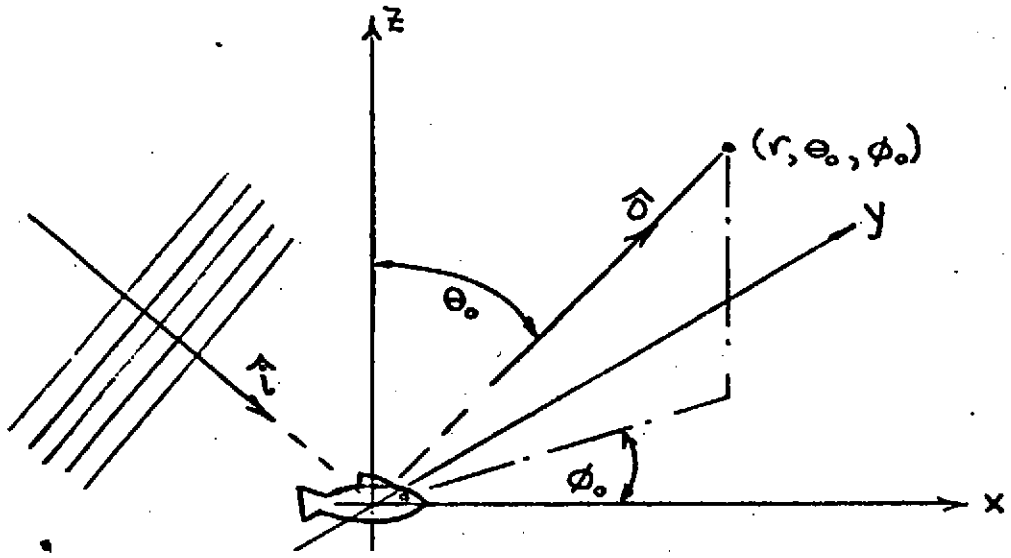

Figure 1 Scattering geometry.

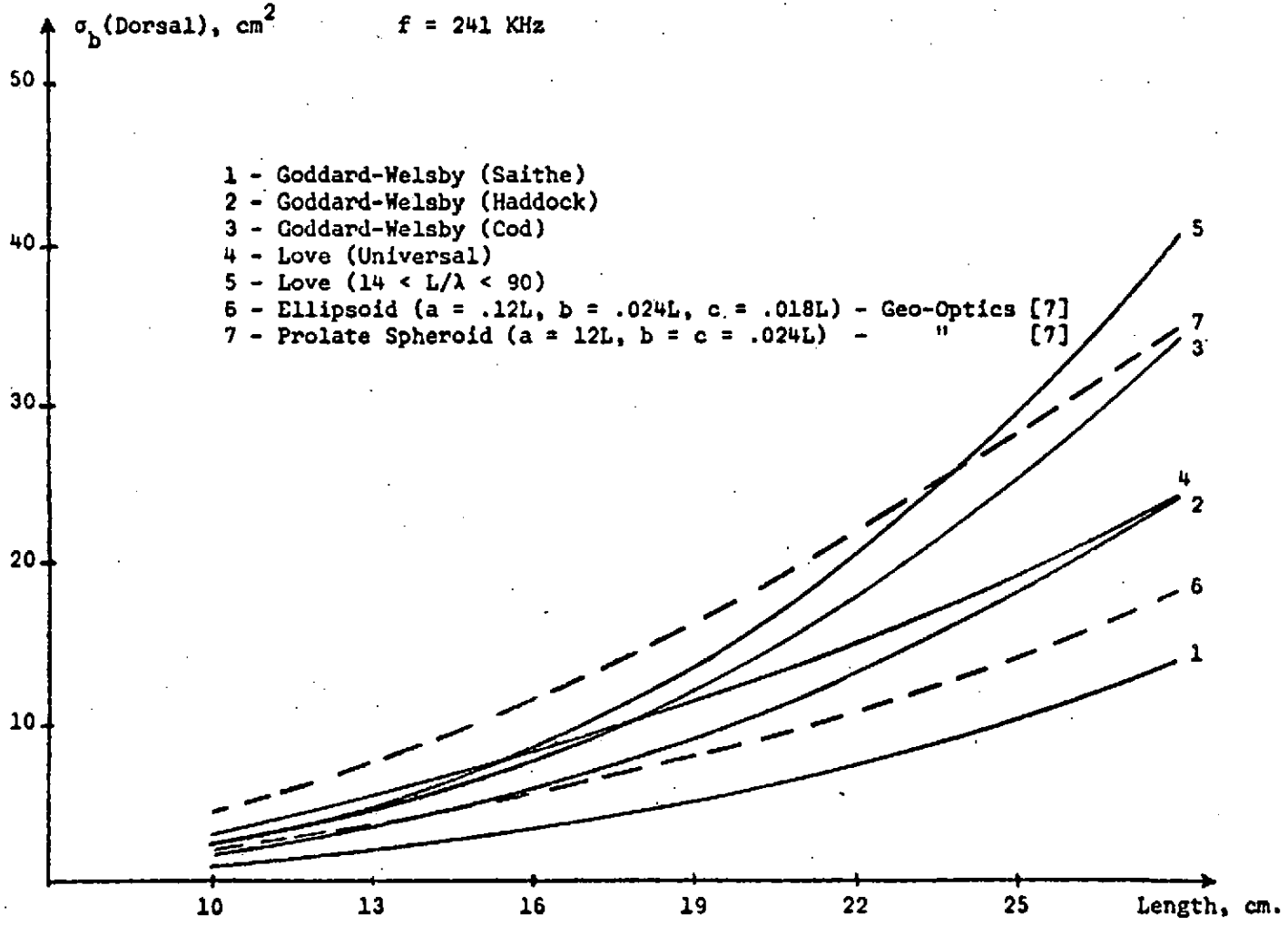

Figure 2 Backscattering cross-sections from various sources.

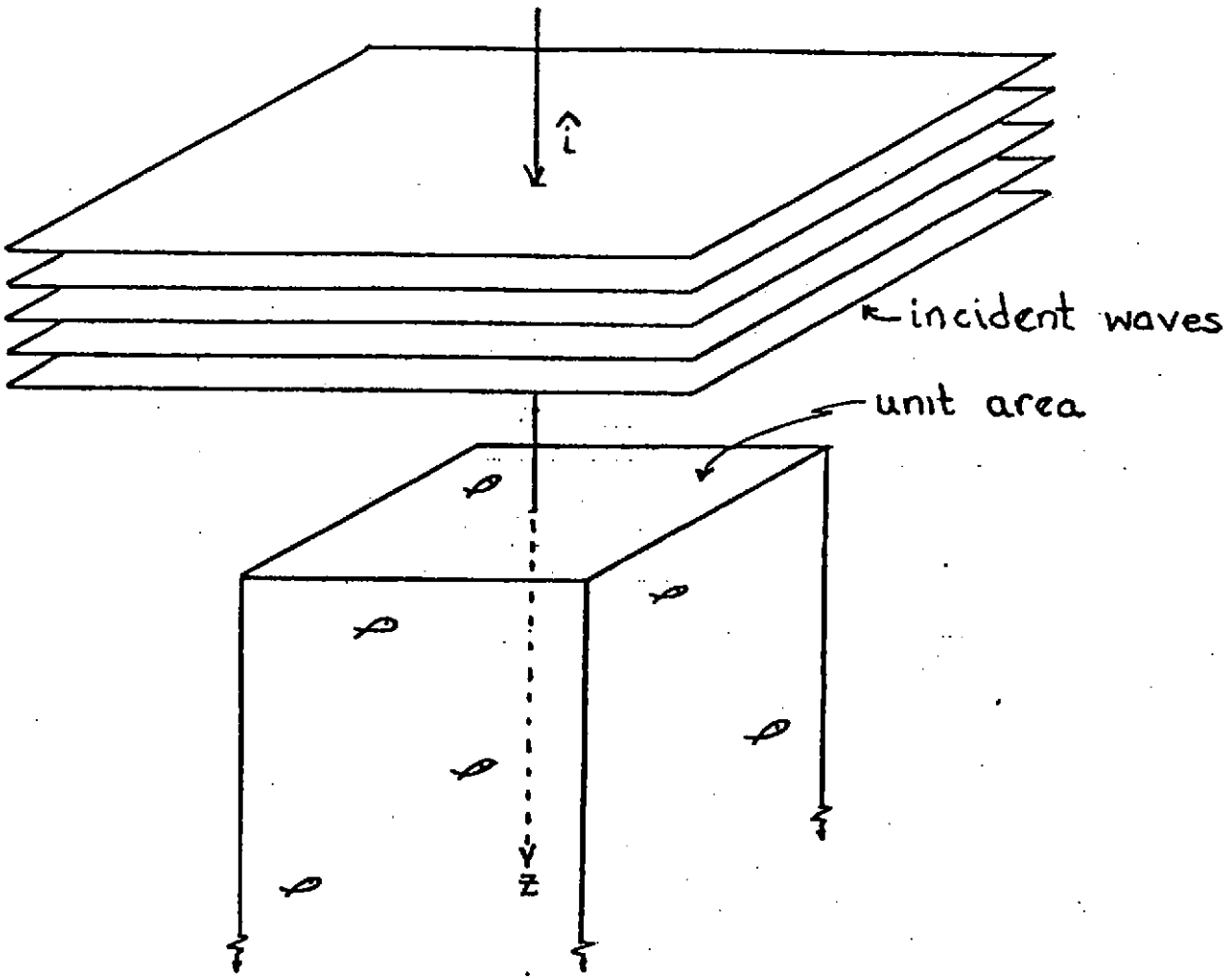

Figure 3 Geometry for computing optical density.

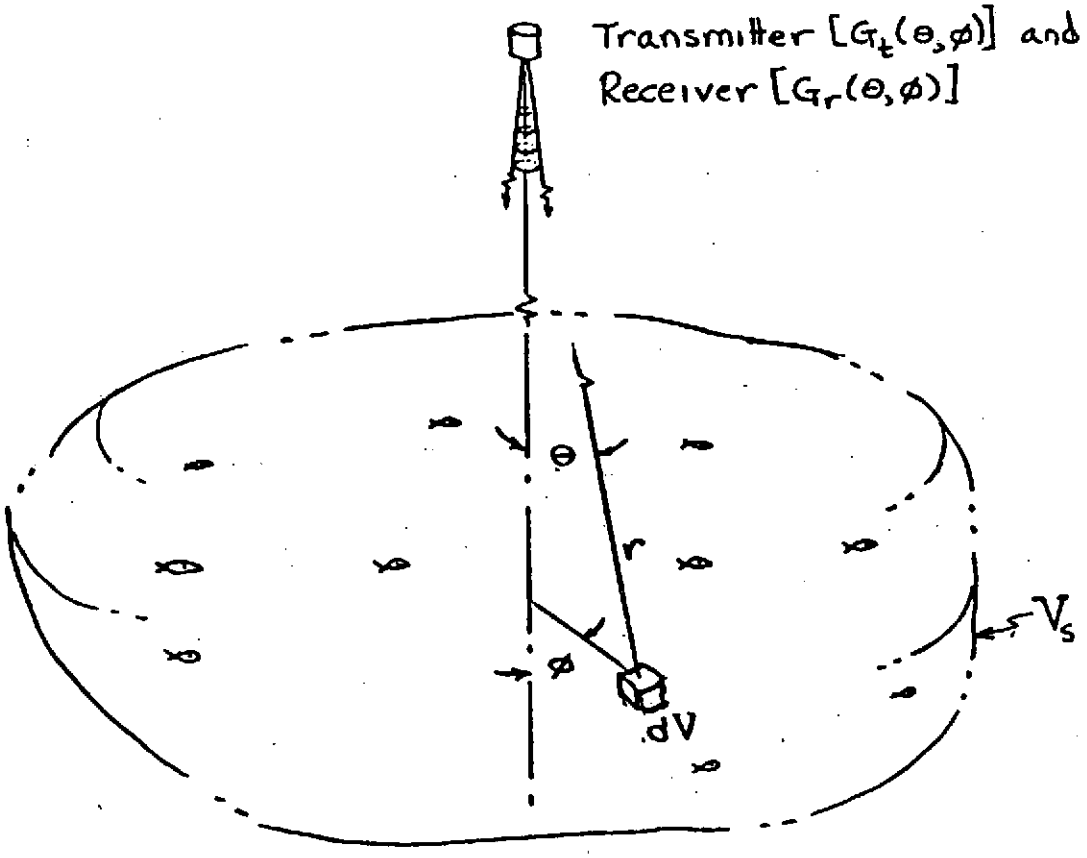

Figure 4 Backscattering geometry for 1st O.M.S.

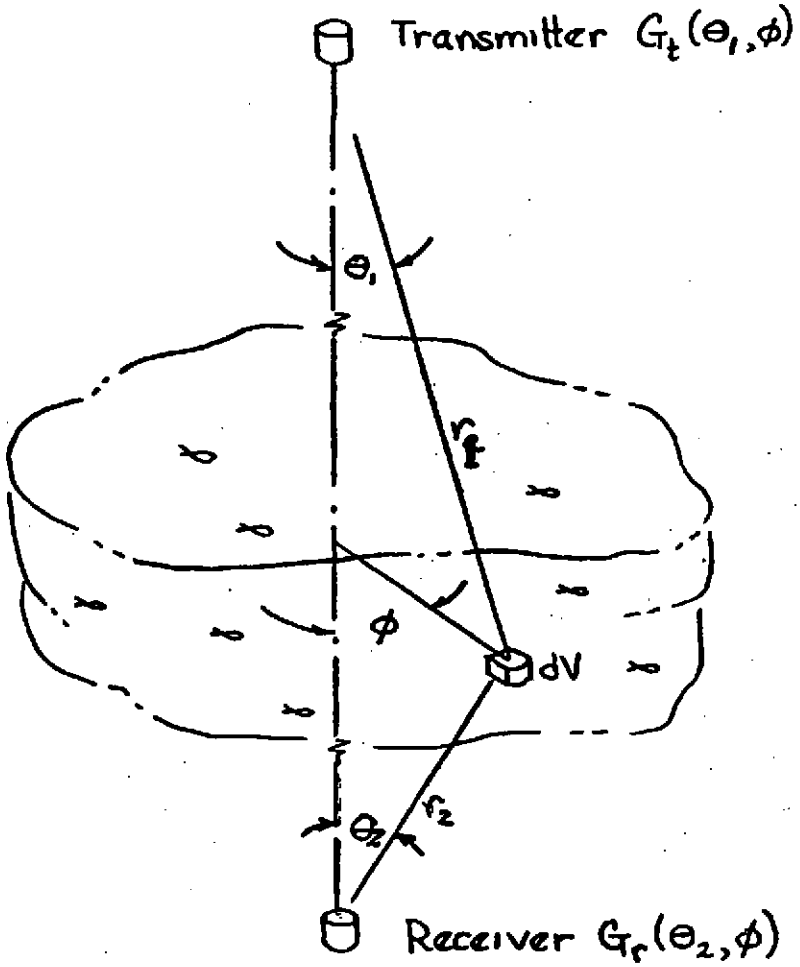

Figure 5 Line-of-sight geometry for 1st O.M.S.

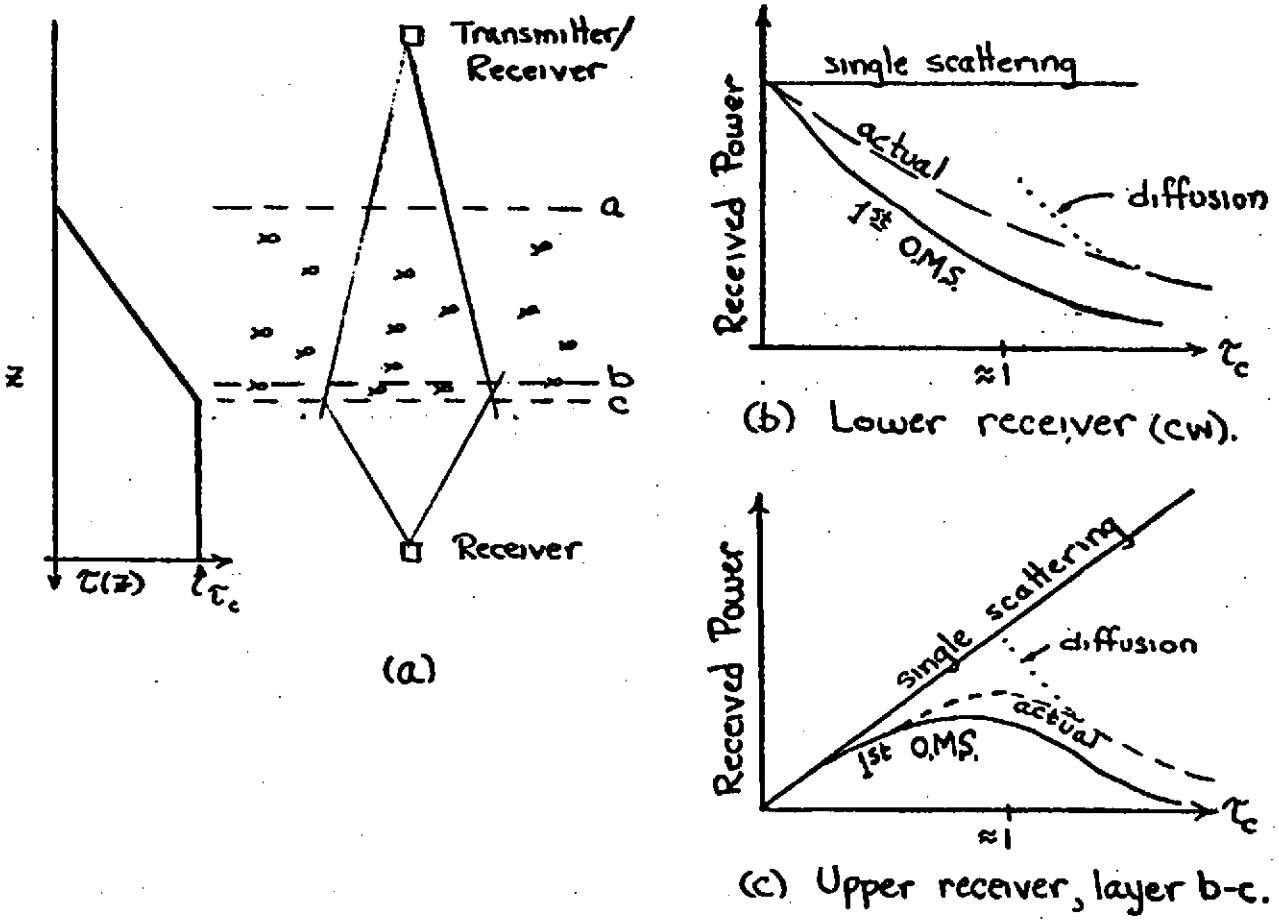

Figure 6 Power received in pulse and CW modes as a function of optical density.

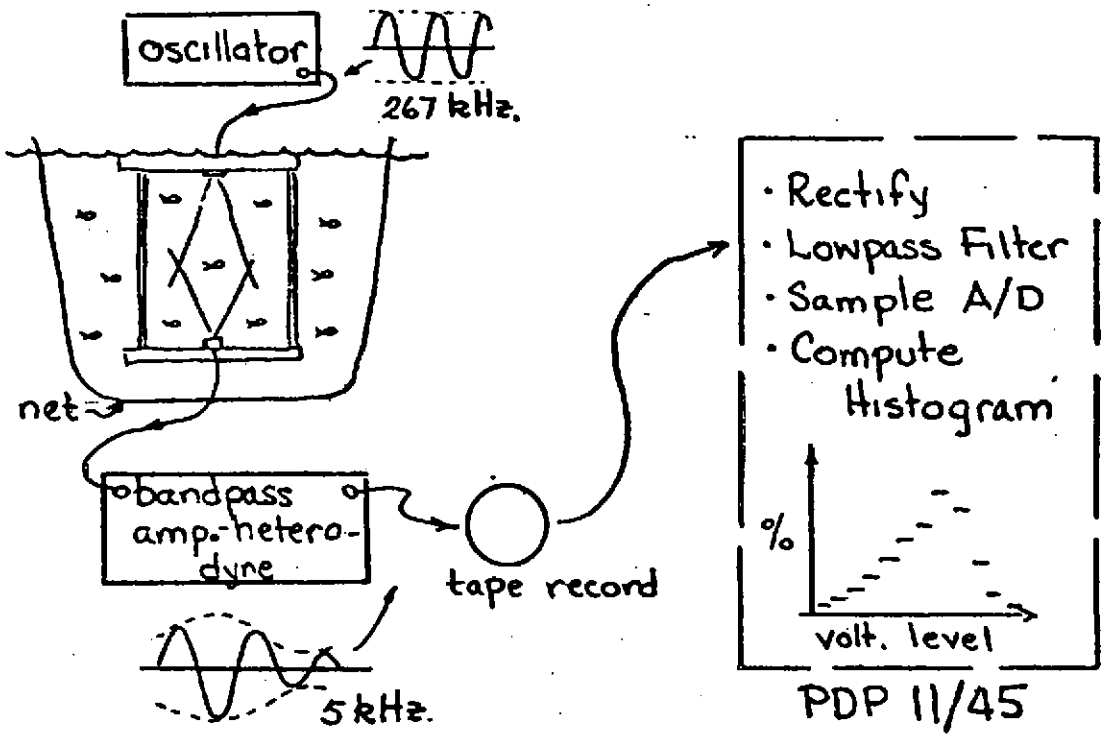

Figure 7 Experimental set-up for CW line-of-sight measurements.

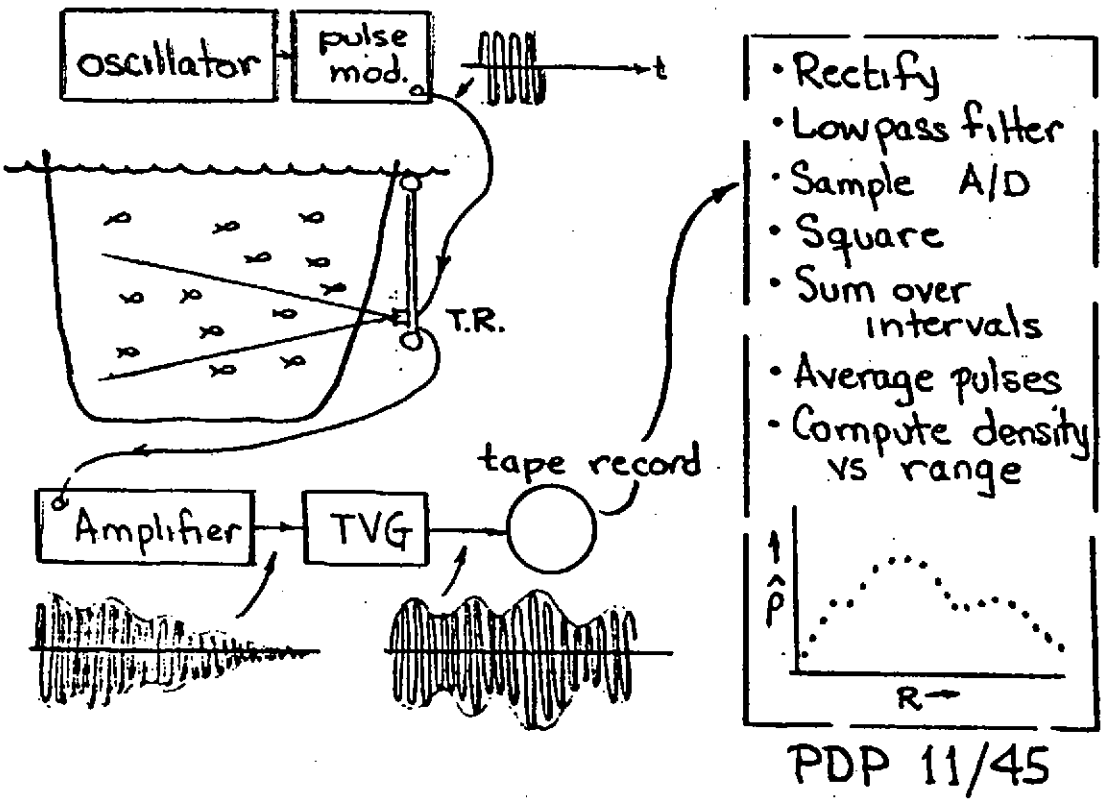

Figure 8 Experimental set-up for pulsed backscatter measurements.

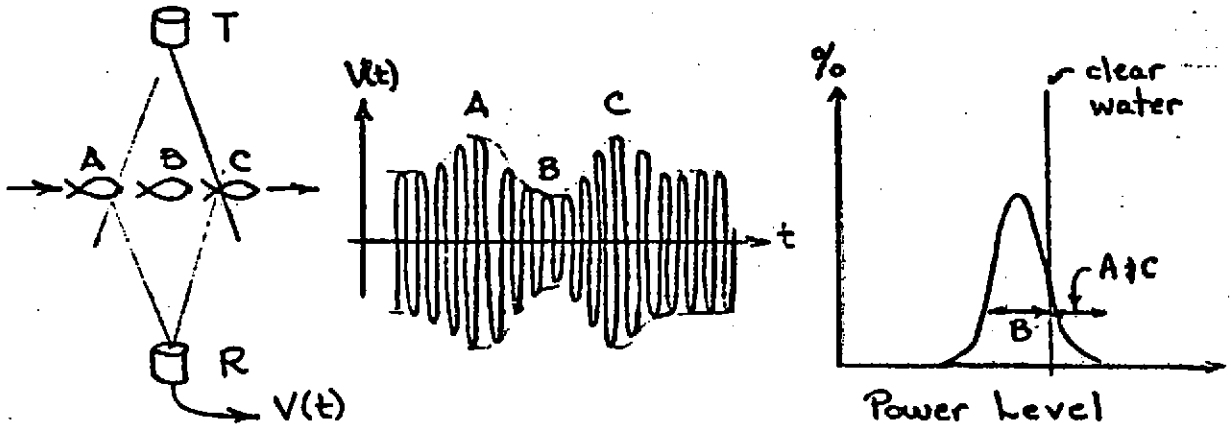

Figure 9 Single fish disturbance and power level histogram.

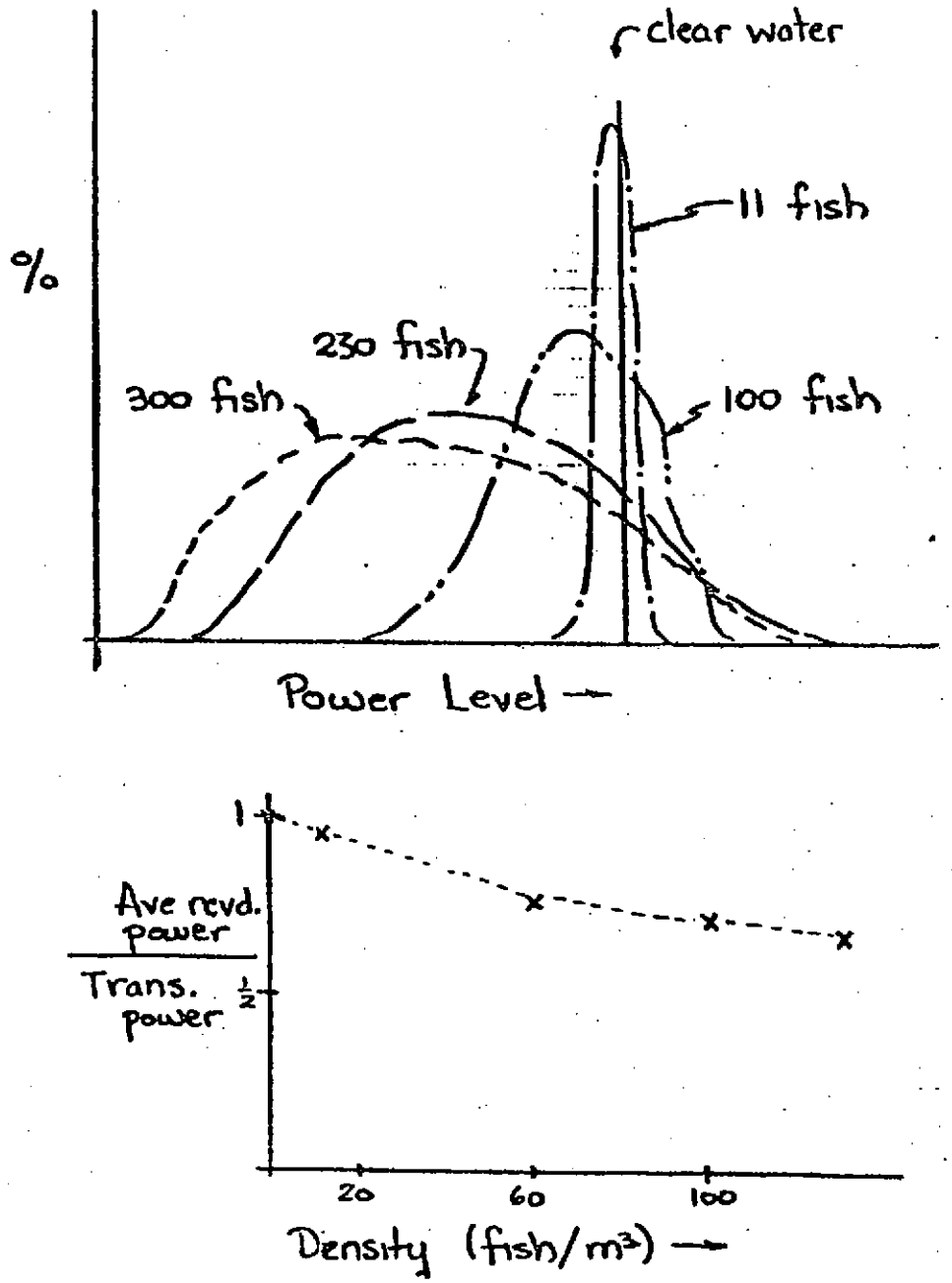

Figure 10 Transmission through "known" densities.

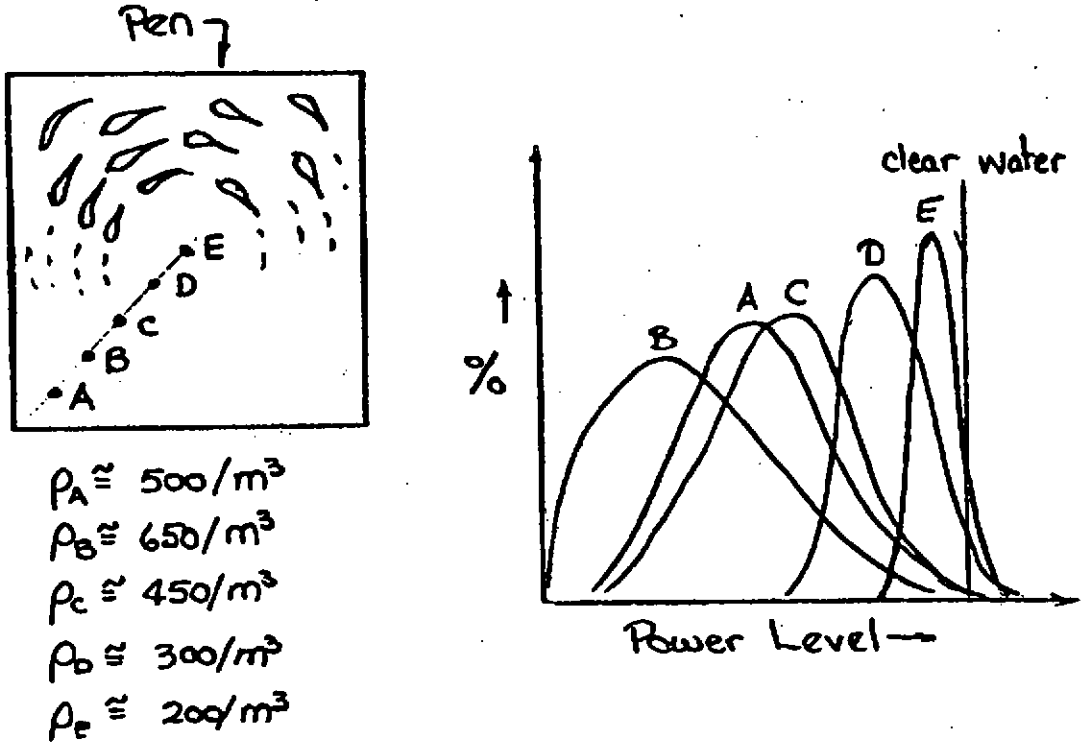

Figure 11 Location dependence of histograms.

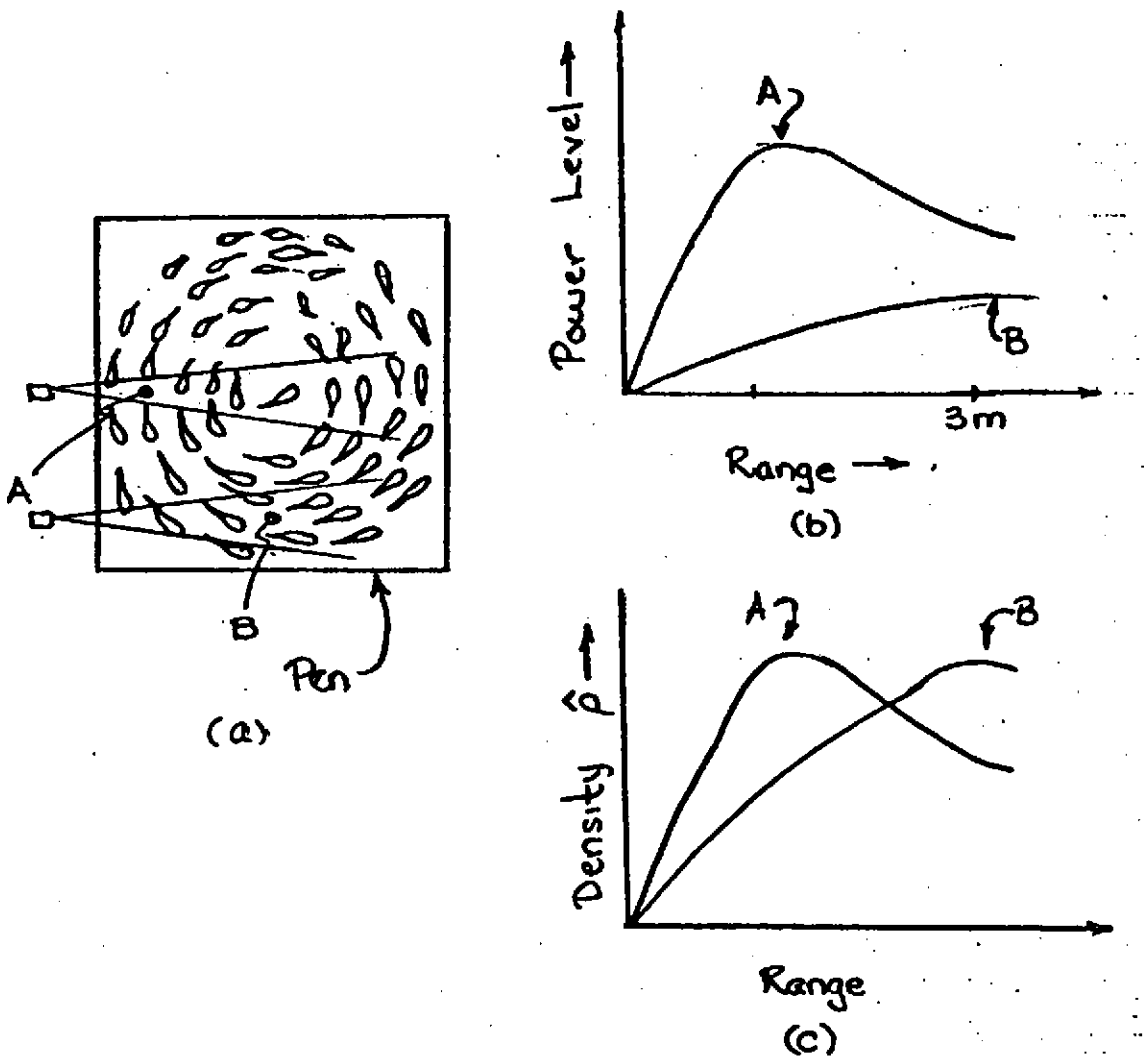

Figure 12 Energy vs range and density vs range as functions of average aspect.

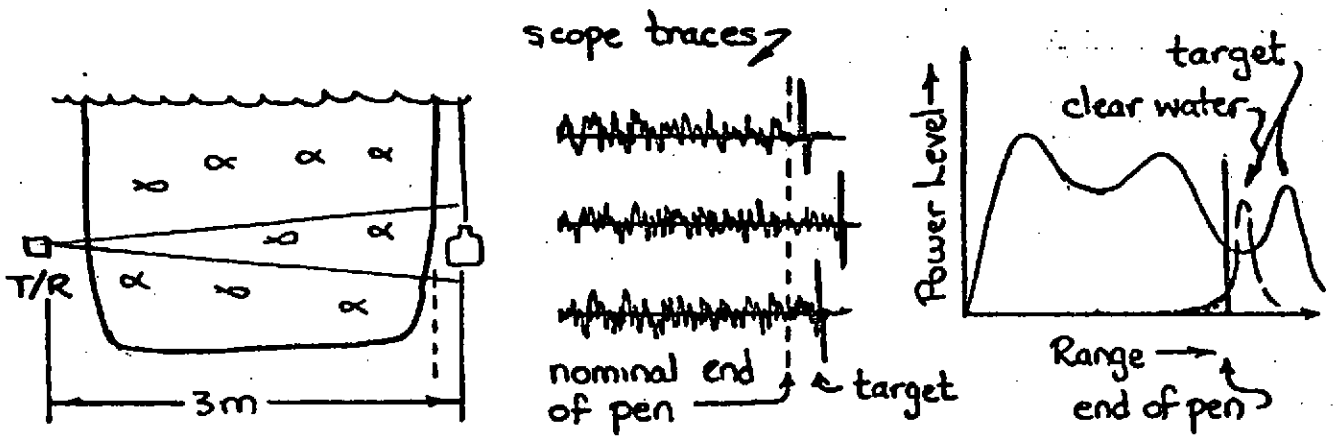

Figure 13 The dancing target.

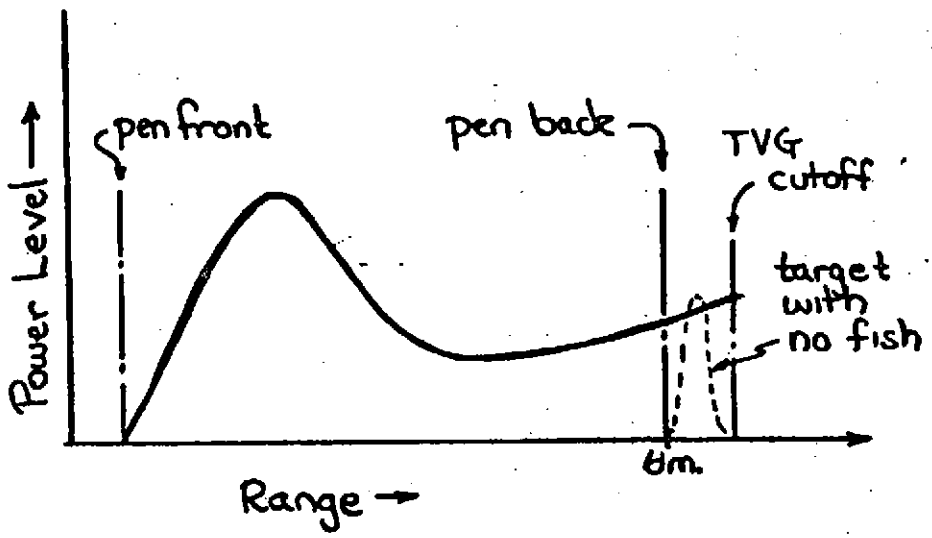

Figure 14 Effects of attenuation and multiple scattering in 6x6x3 meter pen with 18,000 fish at 8 fish per kilogram.

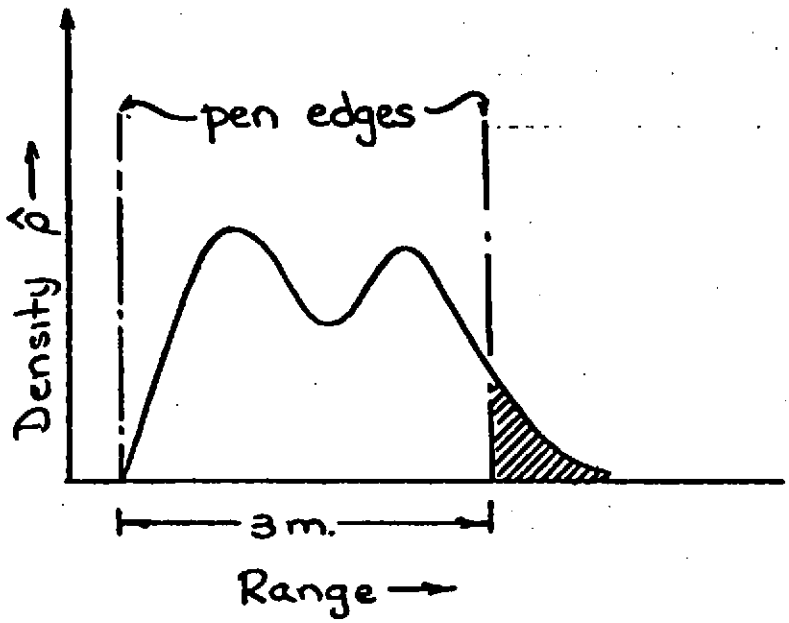

Figure 15 Estimating nonzero density where no fish exist.